

Computational Study of the Correlation of *in-vitro* Antiviral Activities Against SARS-CoV-2 with Different Theoretical Descriptors

M. Díaz^a, D.S. Coll^{a,*}, A. Sierraalta^b, J.L. Zambrano Rouvier^c and F. Salazar^d

^aLaboratorio de Físico Química Teórica de Materiales. Centro de Química. Instituto Venezolano de Investigaciones Científicas. Venezuela

^bLaboratorio de Química Física y Catálisis Computacional. Centro de Química. Instituto Venezolano de Investigaciones Científicas
Venezuela

^cLaboratorio de Biología de Virus. Centro de Microbiología y Biología Celular. Instituto Venezolano de Investigaciones Científicas.
Venezuela

^dLaboratorio de Química Teórica y Computacional. Instituto de la Química Biológica. Universidad de la República. Uruguay

(Received 10 November 2021, Accepted 28 February 2022)

The electrostatic potential ($V(r)$), the average local ionization energy ($I(r)$), the relative hardness (η_{rel}), the electron affinity (EA), the ionization potential (IP), the electronegativity (χ), the hardness (η) and the electrophilicity (ω) were tested as theoretical descriptors of the reported *in-vitro* antiviral activities against SARS-CoV-2 for seven different compounds with the same set of controlled variables: chloroquine, favipiravir, nafamostat, nitazoxanide, penciclovir, remdesivir, rivabirin, in order to obtain information about the electronic nature of the hosting sites in the virus. Results indicate that the hardness of the studied drugs correlates moderately well with the biological activity, which gives some insights to infer in terms of the HSAB principle of Pearson, that the electrostatic interactions must predominate in the virus hosting sites and that these areas have low polarizability. When a multiple correlation analysis is performed, the correlation improves when the conceptual hardness (η), V_{min} , and the molecular volume are considered, which suggests that the interaction of the molecules with the preferred hard hosting sites should be negatively affected by the volume of the selected drug and that V_{min} contributes to the correlation.

Keywords: SARS-CoV-2, Theoretical descriptors, Electrostatic potential. Average Local Ionization Energy, Pearson HSAB principle, chemical hardness

INTRODUCTION

In December 2019, a new coronavirus was reported in the Wuhan district of Hubei province, China [1]. The clinical manifestations observed in the new coronavirus (described as SARS-CoV-2), present a wide spectrum of symptoms ranging from severe pneumonia, fever, cough, dyspnea, acute respiratory stress, multi-organ failure, up to death [2]. In February 2020, the WHO decreed the pandemic and called the disease caused by SARS-CoV-2 as COVID-19 [3].

The SARS-CoV-2 virus belongs to the *Coronaviridae* family, and the *Betacoronavirus* genus. The viral particle is enveloped and has a ≈ 30 Kb, non-segmented, positive-sense single-stranded +ssRNA genome. The genome has numerous open reading frames (ORFs), that codes for four structural proteins: Spike (S), envelope (E), membrane (M), and nucleocapsid (N), and for functional viral enzymes such as RNA-dependent RNA polymerase (RdRP) and proteases. Additionally, the ssRNA genome codes for 16 accessory nonstructural proteins (NSPs) required for viral replication and pathogenesis [4].

Since the appearance of COVID-19 in the world, up to now, more than 220 million people have been infected, of

*Corresponding author. E-mail: dsantiago@ivic.gov.ve

which more than 4.57 million deaths have been caused [5]. The absence of an effective drug has led numerous research groups, as well as pharmaceutical companies, have been working to find a therapy to either treat the disease and control virus replication. A great variety of compounds have been reported, among them, commercial drugs with antiviral activity and others directed towards other microorganisms [6].

The targets of action against SARS-CoV-2 virus, both of the available drugs and novel drugs, are aimed at intervening in the virus-cell interactions that occur during the replicative cycle of SARS-CoV-2. The strategies are 1. The interaction of the ACE2 receptor with SARS-CoV-2 spike protein, 2. Avoid virus particles fusion and uncoating 3. Prevent the primary translation and processing of viral polyprotein and 4. Obstruct the synthesis of viral RNA [7].

Theoretical methods and descriptors (*e.g.* the electrostatic potential ($V(r)$), the average local ionization energy, HOMO-LUMO gap, *etc.*) have been used widely to predict and/or explain the behavior of different species and could represent a guide to its chemical reactivity [8-11]. In an analog way, these theoretical tools were used to predict quantitatively the biological activities of potential drugs and medications and to propose their mechanisms of action, based on the correlations of the theoretical and experimental values [12-15]. Despite several computational studies were performed on this topic [16-20], few of them provide information on the electronic environment of the drug-virus interaction sites. For example, Hempel *et al.* implemented a computational methodology where they combined molecular dynamics calculations and Markov modeling and proposed, based on the average interaction distances of the protein and the drugs of interest, that there was a relationship between the number of Michaelis complexes formed and the inhibitory capacity (IC_{50}) of the drug [20]. This relationship is also present with the EC_{50} reported values for both drugs. However, due to the calculation methodology selected in this work, information on the electronic distribution of the interaction sites of these Michaelis complexes formed cannot be obtained, this study could be complemented with first-principles calculations that would provide this information. The considered drugs may have one or more proposed mechanisms of action, *e.g.* chloroquine (Interference in the endocytic pathway,

blockade of sialic acid receptors, binding site, and prevention of cytokine storm, *etc.*) [21-23], favipiravir (purine analogue) [22,24], nafamostat (inhibition *via* TMPRSS2) [20], nitazoxanide (non-endosomal pathway, endosomal pathway, endosome vesicle formation, and maturation, Inhibition of 3CLpro or PLpro, *etc.* [25-27], penciclovir (DNA chain terminator) [27], remdesivir (targets the machinery responsible for the replication of the viral RNA genome, polymerase stalling) [28,29] and rivabirin (inhibition *via* TMPRSS2 or IMPDH) [30]. However, it is also known that although favorable binding affinities were observed on these works between drug molecules and protein domains, the mechanism of action could not be explained by a single domain interaction. That is why it is of our interest to determine if there is any favorable electronic environment for the interaction of the drugs studied, regardless of the mechanism of action of each of them. In the present work we will quantify eight different theoretical descriptors at HF level: the electrostatic potential ($V(r)$), the average local ionization energy ($I(r)$), the relative hardness (η_{rel}), the electron affinity (EA), the ionization potential (IP), the electronegativity (χ), the hardness (η) and the electrophilicity (ω), for a group of seven drugs previously studied by Wang *et al.* (chloroquine, favipiravir, nafamostat, nitazoxanide, penciclovir, remdesivir, rivabirin) in order to analyze the possible correlation between these intrinsic theoretical quantities and the reported *in-vitro* antiviral activities for each compound, which were obtained with the same set of controlled variables [31], and to retrieve information about the electronic environment of the hosting sites in the virus.

Theoretical Methods

All calculations and geometry optimizations were performed with the Gaussian09 package program using HF/6-311++G** [32]. Frequency calculations of all structures showed that all frequencies were positive indicating that all structures are real minima. The molecular electronic density $\rho(r)$ was obtained from the wfn file [32] and the $V(r)$ was obtained by using the Gaussian09 utility for this purpose.

The active sites susceptibility can be quantified by determining the minimum and maximum values of $V(r)$. These stationary points were localized using a Newton-

Raphson technique [11,33,34]. Bader *et al.* have proposed that the surface of an atom or molecule can reasonably be taken to be the 0.001 a.u. (electrons/bohr³) contour of its electronic density (van der Waals contour); this typically encompasses roughly 98% of its electronic charge and establish a convenient boundary of the outermost (valence) shells [35]. Politzer has shown that by computing $V(r)$ over this isosurface of $\rho(r)$, the susceptibility of molecules to nucleophilic or electrophilic attack can be quantified. Mapping on this isosurface the $V(r)$ values onto colors let us to identify the host sites in which nucleophiles (most positive zone) and electrophiles (most negative zone) should interact. A similar mapping methodology can be applied to molecules for the $I(r)$ function [36].

$\rho(r)$ and $I(r)$ were obtained from the.wfn file [32]. $I(r)$ was calculated according to the Eq. (1):

$$I(r) = \sum_i \frac{\rho_i(r)|\epsilon_i|}{\rho(r)} \quad (1)$$

Where $\rho_i(r)$ is the electronic density of the *i*th molecular orbital at the point *r*, ϵ_i is the orbital energy, and $\rho(r)$ is the total electronic density [8,9]. $I(r)$ could be interpreted as the average energy required to remove an electron from the point *r* in the space of an atom or molecule; this interpretation invokes Koopmans' theorem, a consequence of which is that the ionization energy of an electron can be approximated by the absolute value of its Hartree-Fock orbital energy or its approximate Kohn-Sham orbital energies [37]. It should be noted, however, that the focus is on the point in space, whichever electron may happen to be there, rather than on a particular molecular orbital [38].

The other theoretical descriptors were determined based on Koopmans theorem [39]. Knowing the energy of HOMO and LUMO orbitals, we can correlate these two values with the ionization potential (IP) and with the electron affinity (EA) respectively, by:

$$IP = -\epsilon_{HOMO} \quad (2)$$

$$EA = -\epsilon_{LUMO} \quad (3)$$

The electronegativity (χ), the hardness (η) and the electrophilicity (ω) can be calculated by [40]:

$$\chi = \frac{|IP + EA|}{2} \quad (4)$$

$$\eta = \frac{|IP - EA|}{2} \quad (5)$$

$$\omega = \frac{(IP + EA)^2}{4(IP - EA)} \quad (6)$$

RESULTS AND DISCUSSION

The EC_{50} index (in μM) is presented in Table 1 as a measure of the antiviral activities of the tested drugs against COVID-19 *in-vitro* [31]. The EC_{50} value is the half-maximal effective concentration for a given compound and while smaller is, the greater biological activity it will have. In this table it is clear to see that the compounds activities follow the sequence from best to worst: remdesivir > chloroquine > nitazoxanide > nafamostat > favipiravir > penciclovir > rivabirin.

Table 1. EC_{50} Values for the Tested Drugs Against COVID-19 *in Vitro*

Compound	EC_{50} (μM)
Chloroquine	1.13
Favipiravir	61.88
Nafamostat	22.50
Nitazoxanide	2.12
Penciclovir	95.96
Remdesivir	0.77
Rivabirin	109.50

Although several conformers were considered for each studied compound, only the most stable ones are displayed in Fig. 1. Gray, red, blue, yellow, green, light green, orange and white spheres represent carbon, oxygen, nitrogen, sulphur, chlorine, fluorine, phosphorous, and hydrogen atoms, respectively. Among these structures, there are no special issues to report besides the presence of intramolecular hydrogen bonds in five of the seven drugs (favipiravir, nafamostat, penciclovir, remdesivir, and rivabirin).

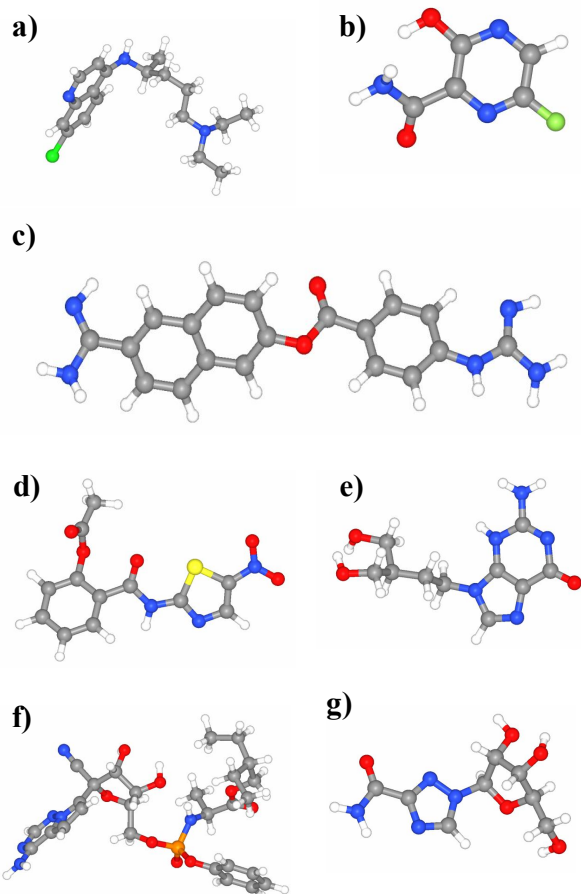


Fig. 1. Optimized geometries of the studied drugs: a) chloroquine, b) favipiravir, c) nafamostat, d) nitazoxanide, e) penciclovir, f) remdesivir, g) rivabirin.

From these optimized structures, we quantified the selected theoretical descriptors. The first one is the mapping of $V(r)$ over 0.001 a.u. isosurface of electron density for the seven compounds which is presented in Fig. 2. The color scale follows the crescent order for the energy values: blue, green, yellow, and red. In this figure are also displayed the $V(r)$ maximum and minimum values for each molecule. The most negatives zones for each molecule are located over the electronic pairs of the nitrogen and oxygen atoms with unsaturated bonds, while the most positives zones are located over the acidic hydrogens bonded to nitrogen atoms as we should expect. From this figure is clear that when the heterogeneous atoms that could contribute to the

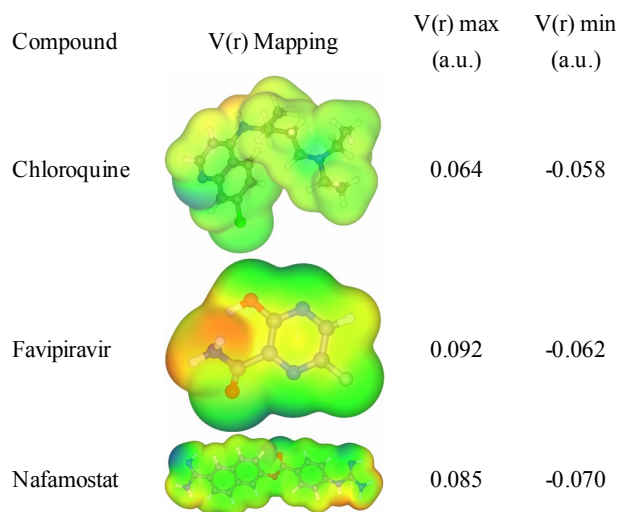


Fig. 2. $V(r)$ mapping for the studied compounds.

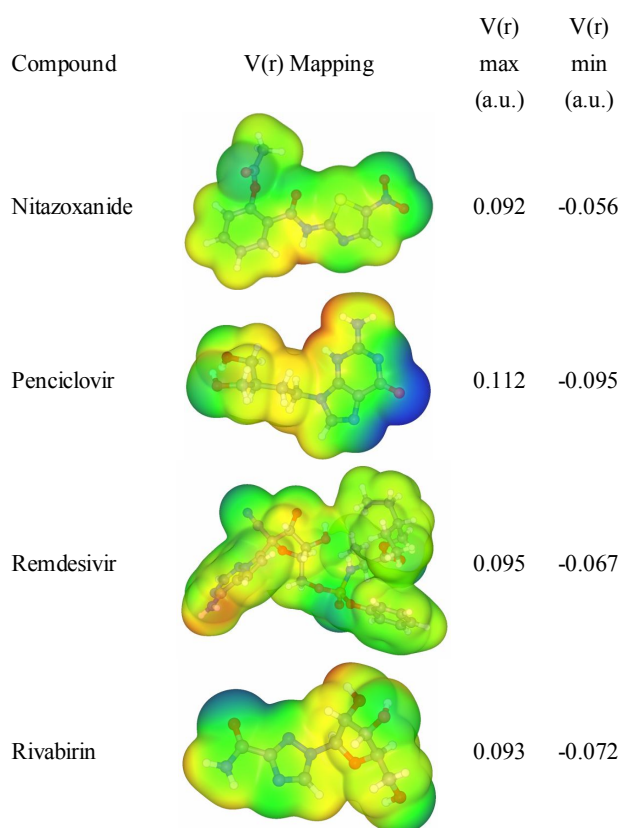


Fig. 2. (Cont.) $V(r)$ mapping for the studied compounds.

electrostatic character of the molecule are forming intramolecular hydrogen bonds, its contribution is greatly

reduced. The amount of this type of atom does not imply a greater electrostatic contribution either. Penciclovir and Remdesivir have the most positive values of the molecules set and the most negative values belong to Penciclovir and Rivabirin. Based on the Hard-Soft/Acid-Base (HSAB) principle of Pearson [41,42], Ayers *et al.* [43,44] proposed that the reactivity of hard molecules (as amines) could be described appropriately by $V(r)$ because this quantity is associated to its electrostatic character and its low polarizability. As the set of molecules studied in this work contains halogens, primary and secondary amines, and alkoxy groups among others we should, at first look, consider it as the hard type and expect the minimum values of $V(r)$ could correlate with the reported biological activity. However when we analyze the correlation between these two quantities the R^2 value for the set of molecules is 0.44, which is poor.

The results for the average local ionization energy mapping are presented in Fig. 3. The color scale follows the same trend as the one described for $V(r)$. Qualitatively, the function distribution over the density isosurface is similar to the one of the $V(r)$ mapping for each case, but the correlation of the I_{\min} with the EC_{50} index is considerably lower ($R^2 = 0.06$).

Despite the low correlation of the average local ionization energy with the EC_{50} , we tested an approach to chemical hardness proposed by Politzer and Murray [45], based on this function. They have proposed that the reciprocal of polarizability as the measure of the chemical hardness of molecules, can be estimated accurately in terms of $I(r)$ and their volumes, by means of the following expression [45]:

$$\eta_{rel} = \frac{I(r)}{V} \quad (7)$$

The volume enclosed by the 0.001 density isosurface was calculated using the AIM-UC code [46] and is included in Table 2 for the studied compounds. With this value and the I_{\min} reported, we calculated the η_{rel} for each molecule (Table 2). The correlation of this quantity with the EC_{50} index has an R^2 value of 0.27, which is better than the one obtained for the I_{\min} , but it is still extremely poor.

Starting from the HOMO and LUMO values of each molecule the rest of the theoretical descriptors were

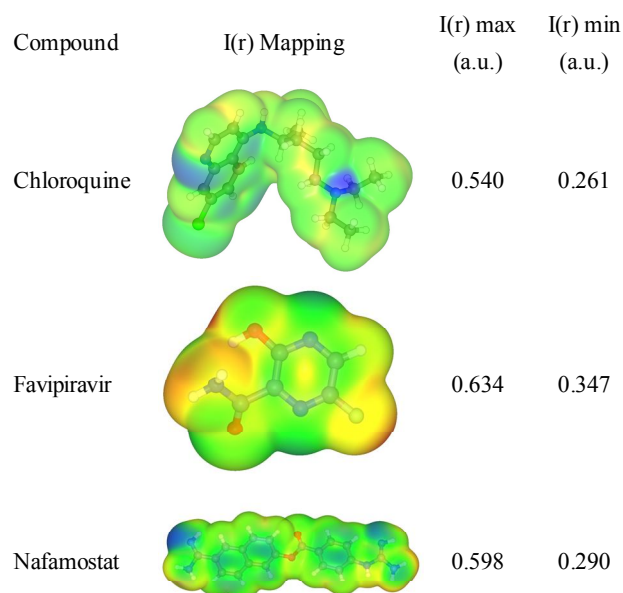


Fig. 3. $I(r)$ mapping for the studied compounds.

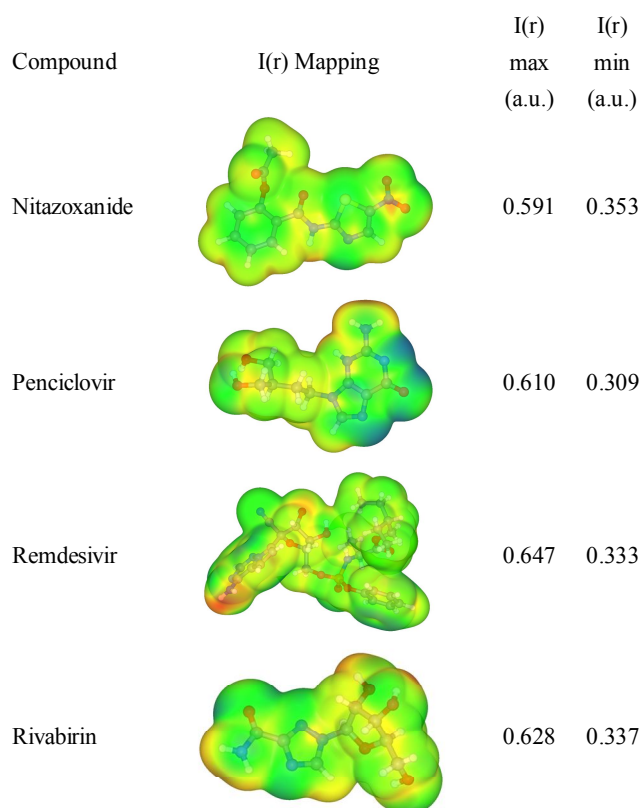


Fig. 3. (Cont.). $I(r)$ mapping for the studied compounds.

Table 2. Molecular Volume and η_{rel} for the Set of Molecules in Atomic Units

Compound	I_{min} (a.u.)	V (bohr ³)	η_{rel}
Chloroquine	0.261	2918.65	0.896×10^{-4}
Favipiravir	0.347	1078.54	3.208×10^{-4}
Nafamostat	0.290	2835.84	1.024×10^{-4}
Nitazoxanide	0.353	2205.11	1.607×10^{-4}
Penciclovir	0.309	2006.19	1.525×10^{-4}
Remdesivir	0.333	4875.60	0.683×10^{-4}
Rivabirin	0.337	1876.74	1.856×10^{-4}

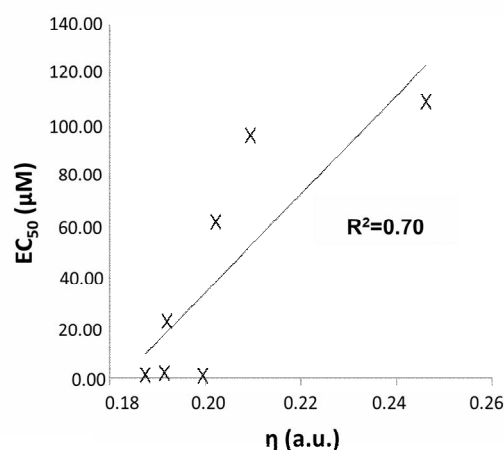
Table 4. The R^2 Value for the Linear Correlation between each Theoretical Descriptor and the EC_{50} Index

Theoretical descriptor	R^2 value
IP	0.31
EA	0.36
χ	~ 0.00
η	0.70
ω	0.05
V_{min}	0.44
I_{min}	0.06
η_{rel}	0.27

calculated with formulas (2) to (6). The magnitudes of the Ionization Potential (IP), the Electronic Affinity (EA), the electronegativity (χ), the conceptual hardness (η) and the electrophilicity (ω) are presented in Table 3 together with the reported EC_{50} values and the ones of the $V(r)$ minimum (V_{min}). All quantities are presented in atomic units of energy, excepting the EC_{50} index which is in μM .

The correlation between each theoretical descriptor and the EC_{50} index were studied and the values of R^2 are presented in Table 4.

Among the eight descriptors studied, the one which shows the best correlation is the conceptual hardness (η). The graph for this distribution is presented in Fig. 4. Although the value correlation is not well enough to consider it acceptable, it could give us some insights into the electronic nature of the hosting sites in the virus. According to the HSAB principle, hard species will prefer to interact with

**Fig. 4.** Correlation between the EC_{50} index (μM) and the conceptual hardness (a.u.) for the studied compounds.**Table 3.** Theoretical Descriptors Values for the Set of Molecules in Atomic Units. The EC_{50} Index is also Presented

Compound	V_{min}	I_{min}	η_{rel}	IP	EA	χ	η	ω	EC_{50} (μM)
Chloroquine	-0.058	0.261	0.896×10^{-4}	0.303	0.072	0.116	0.188	0.036	1.13
Favipiravir	-0.062	0.347	3.208×10^{-4}	0.357	0.047	0.155	0.202	0.060	61.88
Nafamostat	-0.071	0.290	1.024×10^{-4}	0.302	0.082	0.110	0.192	0.032	22.50
Nitazoxanide	-0.056	0.353	1.607×10^{-4}	0.351	0.032	0.160	0.192	0.066	2.12
Penciclovir	-0.095	0.309	1.525×10^{-4}	0.319	0.100	0.110	0.210	0.029	95.96
Remdesivir	-0.067	0.333	0.683×10^{-4}	0.320	0.079	0.121	0.200	0.036	0.77
Rivabirin	-0.072	0.337	1.856×10^{-4}	0.384	0.109	0.138	0.246	0.038	109.50

hard species, in our case the most biologically active compounds will interact more effectively in hard zones of the virus that is, hosting areas where electrostatic interactions should predominate and therefore in order to analyze the influence of the molecular volume in the interaction between the virus and the selected drug and to determine if there are other variables intervening in the correlation with the EC₅₀, we performed a multiple correlation analysis.

From this analysis, we found a better correlation between the EC₅₀ values and the rest of the variables. When we analyze the contribution that the conceptual hardness (η), V_{min}, and the molecular volume have on the EC₅₀ variability, we obtain a correlation with R² = 0.983 (with a Q² = 0.832). The equation for this model is:

$$EC_{50} (\mu M) = -284.4 - 1487.8 * (V_{min}) + 1293.9 * (\eta) - 15.8 * (\text{Volume})$$

Given the R² value, these 3 variables explain 98% of the variability of the dependent variable EC₅₀ (μ M). Given the p value (p = 0.004) associated with the F statistic calculated (56,27), and given the 5% level of significance, the information provided by the explanatory variables is significantly better than that which could be provided by the mean alone. The most influential variable is the conceptual hardness (η).

This result suggests that the interaction of the molecules with the preferred hard hosting sites should be negatively affected by the volume of the selected drug. The larger the volume, the worse the interaction between the drug and the hosting site. On the other hand, it can also be seen that V_{min} contributes positively to the hardness of the hosting site.

CONCLUSIONS

The structures of seven different compounds (chloroquine, favipiravir, nafamostat, nitazoxanide, penciclovir, remdesivir, rivabirin) were geometrically optimized. From each of these structures, eight theoretical descriptors were determined in order to analyze a possible correlation between these quantities and the reported *in-vitro* antiviral activities against SARS-CoV-2. Results

show a poor correlation with the average local ionization energy (I(r)), the relative hardness (η_{rel}), the Ionization Potential (IP), the Electronic Affinity (EA), the electronegativity (χ), the electrophilicity (ω) and V_{min} descriptors and a moderate correlation with the hardness (η). These results give some insights to infer in terms of the HSAB principle of Pearson, that the electrostatic interactions must predominate in the virus hosting sites and that these areas have low polarizability. The multiple correlation analysis performed between the EC₅₀, the conceptual hardness, V_{min}, and the molecular volume for each compound, suggests that the interaction of the molecules with the preferred hard hosting sites should be negatively affected by the volume of the selected drug and that the values of V_{min}, which is also associated to the hardness, contribute positively to the correlation.

FUNDINGS

This research did not receive any specific grant from funding agencies in the public, commercial, or not-for-profit sectors.

REFERENCES

- [1] Huang, C.; Wang Y.; Li X.; Ren, L.; Zhao, J.; Hu, Y.; Zhang, L.; Fan, G.; Xu, J.; Gu, X.; Cheng, Z.; Yu, T.; Xia, J.; Wei, Y.; Wu, W.; Xie, X.; Yin, W.; Li, H.; Liu, M.; Xiao, Y.; Gao, H.; Guo, L.; Xie, J.; Wang, G.; Jiang, R.; Gao, Z.; Jin, Q.; Wang, J.; Cao, B., Clinical features of patients infected with 2019 novel coronavirus in Wuhan, *China. Lancet* **2020**, *395*, 497-506, DOI: 10.1016/S0140-6736(20)30183-5.
- [2] Zhu, N.; Zhang, D.; Wang, W.; Li, X.; Yang, B.; Song, J.; Zhao, X.; Huang, B.; Shi, W.; Lu, R.; Niu, P.; Zhan, F.; Ma, X.; Wang, D.; Xu, W.; Wu, G.; Gao, G.; Tan, W., A novel coronavirus from patients with pneumonia in China. *N. Engl. J. Med.* **2020**, *382*, 727-733, DOI: 10.1056/NEJMoa2001017.
- [3] World Health Organization. 2020. <https://www.who.int/dg/speeches/detail/who-director-general-s-remarks-at-the-media-briefing-on-2019-ncov-on-11-february-2020>.
- [4] Chan, J; Kok, K.; Zhu, Z; Chu, H; To, K.; Yuan, S.;

- Yuen, K., Genomic characterization of the 2019 novel human-pathogenic coronavirus isolated from a patient with atypical pneumonia after visiting Wuhan. *Emerg. Microbes Infect.* **2020**, *9*, 221-236, DOI: 10.1080/22221751.2020.1719902.
- [5] Center for Systems Science and Engineering (CSSE) at Johns Hopkins University (JHU) COVID-19 Dashboard. ArcGIS. Johns Hopkins University. Retrieved 6 September 2021.
- [6] Lu, H., Drug treatment options for the 2019-new coronavirus (2019-nCoV). *BioSci. Trends* **2020**, *14*, 69-71, DOI: 10.5582/bst.2020.01020.
- [7] Ortega, J.; Zambrano, J.; Jastrzebska, B.; Liprandi, F.; Rangel, H.; Pujol, F., Understanding severe acute respiratory syndrome coronavirus 2 replication to design efficient drug combination therapies. *Intervirology* **2020**, *63*, 2-9, DOI: 10.1159/000512141.
- [8] Aray, Y.; Rodríguez, J.; Coll, D. S.; Gonzalez, C.; Márquez, M., Exploring the nature of wetting by water of surfaces of alkane-amidethiols adsorbed on gold using the electrostatic potential topology. *J. Phys. Chem. B* **2004**, *108*, 18942-18948, DOI: 10.1021/jp047278o.
- [9] Coll, D. S.; Vidal, A.; Rodríguez, J.; Ocando-Mavárez, E.; Añez, R.; Sierralta, A., A simple method for the determination of the Tolman electronic parameter of different phosphorus containing ligands, by means of the average local ionization energy. *Inorganica Chimica Acta* **2015**, *436*, 163-168, DOI: 10.1016/j.ica.2015.08.003.
- [10] Aray, Y.; Rodríguez, J.; Coll, S.; Rodríguez-Arias, E. N.; Vega, D., Nature of the Lewis acid sites on molybdenum and ruthenium sulfides: An electrostatic potential study. *J. Phys. Chem. B* **2005**, *109*, 23564-23570, DOI: 10.1021/jp054097t.
- [11] Aray, Y.; Marquez, M.; Rodríguez, J.; Coll, S.; Simon-Manso, Y.; Gonzalez, C., Electrostatics for exploring the nature of water adsorption on the laponite sheets' surface. *J. Phys. Chem. B* **2003**, *107*, 8946-8952, DOI: 10.1021/jp0302257.
- [12] Chiari, L.; Da Silva, A. P.; De Oliveira, A.; Lipinskia, C.; Honório, K.; Da Silva, A. B., Drug design of new sigma-1 antagonists against neuropathic pain: A QSAR study using partial least squares and artificial neural networks. *J. Mol. Struct.* **2021**, *1223*, 129156, DOI: 10.1016/j.molstruc.2020.129156.
- [13] Alcala, A.; Hernandez-Bravo, R.; Medina, F.; Coll, D. S.; Zambrano, J.; Del Angel, R.; Ludert, J., The dengue virus non-structural protein 1 (NS1) is secreted from infected mosquito cells *via* a non-classical caveolin-1-dependent pathway. *J. Gen. Virol.* **2017**, *98*, 2088-2099, DOI: 10.1099/jgv.0.000881.
- [14] Sánchez, O.; González, S.; Higuera-Padilla, A.; León, Y.; Coll, D.; Fernández, M.; Taylor, P.; Urdanibia, I.; Rangel, H.; Ortega, J.; Castro, W.; Goite, M., Remarkable *in vitro* anti-HIV activity of new silver(I)-and gold(I)-N-heterocyclic carbene complexes. Synthesis, DNA binding and biological evaluation. *Polyhedron* **2016**, *110*, 14-23, 10.1016/j.poly.2016.02.012.
- [15] El Khatabi, K.; El-mernissi, R.; Aanouz, I.; Ajana, M. A.; Lakhliifi, T.; Shahinozaman, M.; Bouachrine, M., Benzimidazole derivatives in identifying novel acetylcholinesterase inhibitors: A combination of 3D-QSAR, docking, and molecular dynamics simulation. *Phys. Chem. Res.* **2022**, *10*, 237-249, DOI: 10.22036/PCR.2021.277306.1895.
- [16] Singh, A. K.; Singh, A.; Shaikh, A.; Singh, R.; Misra, A., Chloroquine and hydroxychloroquine in the treatment of COVID-19 with or without diabetes: a systematic search and a narrative review with a special reference to India and other developing countries. *Diabetes Metab. Syndr. Clin. Res. Rev.*, **2020**, *14*, 241-246, DOI: 10.1016/j.dsx.2020.03.011.
- [17] Belhassan, A.; Zaki, H.; Chtita, S.; Alaqrbeh, S.; Alsakhen, N.; Benlyas, M.; Lakhliifi, T.; Bouachrine, M., Camphor, artemisinin and sumac phytochemicals as inhibitors against COVID-19: Computational approach. *Comp. Bio. Med.*, **2021**, *136*, 104758, DOI: 10.1016/j.compbio.2021.104758.
- [18] Belhassan, A.; En-nahli, F.; Zaki, H.; Lakhliifi, T.; Bouachrine, M., Assessment of effective imidazole derivatives against SARS-CoV-2 main protease through computational approach. *Life Sci.* **2020**, *118469*, DOI: 10.1016/j.lfs.2020.118469.
- [19] El Khatabi, K.; Aanouz, I.; Alaqrbeh, M.; Ajana, M. A.; Lakhliifi, T.; Bouachrine, M., Molecular docking,

- molecular dynamics simulation, and ADMET analysis of levamisole derivatives against the SARS-CoV-2 main protease (M-Pro). *Bioimpacts*, **2021**, 7-7, DOI: 10.34172/bi.2021.22143.
- [20] Hempel, T.; Raich, L.; Olsson, S.; Azouz, N. P.; Klingler, A. M.; Rothenberg, M. E.; Noé, F., Molecular mechanism of SARS-CoV-2 cell entry inhibition *via* TMPRSS2 by Camostat and Nafamostat mesylate. *BioRxiv.*, **2020**, 1-10, DOI: 10.1101/2020.07.21.214098.
- [21] Satarker, S.; Ahuja, T.; Banerjee, M.; Balaji V.; Dogra, S.; Agarwal, T.; Nampoothiri, M., Hydroxychloroquine in COVID-19: Potential mechanism of action against SARS-CoV-2. *Curr. Pharmacol. Rep.*, **2020**, 6, 203-211, DOI: 10.1007/s40495-020-00231-8
- [22] Pavlova, V.; Hristova, S.; Uzunova K.; Vekov, T., A review on the mechanism of action of favipiravir and hydroxychloroquine in COVID-19. *Res. Rev. Insights*, **2021**, 5, 1-7, DOI: 10.15761/VDT.1000167.
- [23] Matrosovich, M.; Herrler, G.; Klenk, H. D., Sialic Acid Receptors of Viruses. In: Gerardy-Schahn, R., Delannoy, P., von Itzstein M. (Eds.), SialoGlyco Chemistry and Biology II. *Topics in Current Chemistry*, **2013**, 367. Springer, Cham., DOI: 10.1007/128_2013_466.
- [24] Dabbous, H. M., Abd-Elsalam, S.; El-Sayed, M. H.; Sherief, A. F.; Ebeid, F.; El Ghafar, M. S. A.; Soliman, S.; Elbahnasawy, M.; Badawi, R.; Tageldin, M. A., Retracted Article: Efficacy of favipiravir in COVID-19 treatment: a multi-center randomized study. *Arch. Virol.*, **2021**, 166, 949-954, DOI: 10.1007/s00705-021-04956-9.
- [25] Lokhande, A. S.; Devarajan, P. V., A review on possible mechanistic insights of Nitazoxanide for repurposing in COVID-19. *Eur. J. Pharm.*, **2021**, 891, 173748. DOI: 10.1016/j.ejphar.2020.173748.
- [26] Blum, V. F.; Cimerman, S.; Hunter, J. R.; Tierno, P.; Lacerda, A.; Soeiro, A.; Cardoso, F.; Bellei, N. C.; Maricato, J.; Mantovani, N.; Vassao, M.; Dias, D.; Galinskas, J.; Janini, L.; Santos-Oliveira, J. R.; Da-Cruz, A. M.; Diaz, R. S., Nitazoxanide superiority to placebo to treat moderate COVID-19 - A Pilot prove of concept randomized double-blind clinical trial. *Eclinical Medicine*, **2021**, 37, DOI: 10.1016/j.eclinm.2021.100981.
- [27] Kausar, S.; Said Khan, F.; Ishaq Mujeeb Ur Rehman, M.; Akram, M.; Riaz, M.; Rasool, G.; Hamid Khan, A.; Saleem, I.; Shamim, S.; Malik, A., A review: Mechanism of action of antiviral drugs. *Int. J. Immunopath. Pharm.*, **2021**, 35, 20587384211002621. DOI: 10.1177/20587384211002621.
- [28] Kokic, G.; Hillen, H. S.; Tegunov, D.; Dienemann, C.; Seitz, F.; Schmitzova, J.; Farnung, L.; Siewert, A.; Höbartner, C.; Cramer, P., Mechanism of SARS-CoV-2 polymerase stalling by remdesivir. *Nat. Commun.* **2021**, 12, 279, DOI: 10.1038/s41467-020-20542-0.
- [29] Malin, J. J., Suárez, I.; Priesner, V.; Fätkenheuer, G.; Rybniker, J., Remdesivir against COVID-19 and other viral diseases. *Clinic. Microb. Rev.*, **2020**, 34, e00162-20. DOI: 10.1128/CMR.00162-20.
- [30] Unal, M. A.; Bitirim, C. A.; Summak, G. Y.; Bereketoglu, S.; Zeytin, I. C.; Besbinar, O.; Gurcan, C.; Aydos, D.; Goksoy, E.; Kocakaya, E.; Eran, Z.; Murat, M.; Demir, N.; Ozer, Z. B. A.; Somers, J.; Demir, E.; Nazir, H.; Ozkan, S. A.; Ozkul, A.; Azap, A.; Yilmazer, A.; Akcali, K. C., Ribavirin shows antiviral activity against SARS-CoV-2 and downregulates the activity of TMPRSS2 and the expression of ACE2 *in vitro*. *Can. J. Phys. Pharm.*, **2020**, 99, 449-460. DOI: 10.1139/cjpp-2020-0734.
- [31] Wang, M.; Cao, R.; Zhang, L.; Yang, X.; Liu, J.; Xu, M.; Shi, Z.; Hu, Z.; Zhong, W.; Xiao, G., Remdesivir and chloroquine effectively inhibit the recently emerged novel coronavirus (2019-nCoV) *in vitro*. *Cell Res.* **2020**, 30, 269-271, DOI: 10.1038/s41422-020-0282-0.
- [32] Gaussian 09, Revision D.01, Frisch, M. J.; Trucks, G. W.; Schlegel, H. B.; Scuseria, G. E.; Robb, M. A.; Cheeseman, J. R.; Scalmani, G.; Barone, V.; Mennucci, B.; Petersson, G. A.; Nakatsuji, H.; Caricato, M.; Li, X.; Hratchian, H. P.; Izmaylov, A. F.; Bloino, J.; Zheng, G.; Sonnenberg, J. L.; Hada, M.; Ehara, M.; Toyota, K.; Fukuda, R.; Hasegawa, J.; Ishida, M.; Nakajima, T.; Honda, Y.; Kitao, O.; Nakai, H.; Vreven, T.; Montgomery, J. A., Jr.; Peralta, J. E.; Ogliaro, F.; Bearpark, M.; Heyd, J. J.; Brothers, E.; Kudin, K. N.; Staroverov, V. N.; Kobayashi, R.;

- Normand, J.; Raghavachari, K.; Rendell, A.; Burant, J. C.; Iyengar, S. S.; Tomasi, J.; Cossi, M.; Rega, N.; Millam, M. J.; Klene, M.; Knox, J. E.; Cross, J. B.; Bakken, V.; Adamo, C.; Jaramillo, J.; Gomperts, R.; Stratmann, R. E.; Yazyev, O.; Austin, A. J.; Cammi, R.; Pomelli, C.; Ochterski, J. W.; Martin, R. L.; Morokuma, K.; Zakrzewski, V. G.; Voth, G. A.; Salvador, P.; Dannenberg, J. J.; Dapprich, S.; Daniels, A. D.; Farkas, Ö.; Foresman, J. B.; Ortiz, J. V.; Cioslowski, J.; Fox, D. J., Gaussian, Inc., Wallingford CT, 2009.
- [33] Vega, D.; Abache, J.; Coll, D., A fast and memory saving marching cubes 33 implementation with the correct interior test. *J. Comput. Graph. Tech.* **2019**, *8*, 1-18, <http://jcgt.org/published/0008/03/01/>.
- [34] Aray, Y.; Rodriguez, J.; Vidal, A. B.; Coll, S., Nature of the NiMoS catalyst edge sites: An atom in molecules theory and electrostatic potential studies. *J. Mol. Cat. A-Chem.* **2007**, *271*, 105-116, DOI: 10.1016/j.molcata.2007.02.016.
- [35] Bloor, J. E.; Gillespie, R.; Popelier, P., Chemical bonding and molecular geometry: From lewis to electron densities. *Found. Chem.* **2002**, *4*, 241-247, DOI: 10.1023/A:1020691330843.
- [36] Politzer, P.; Murray, J. S.; Grice, M. E., Electronegativity and average local ionization energy. *Collect. Czech. Chem. Commun.* **2005**, *70*, 550-558, DOI: 10.1135/cccc20050550.
- [37] Politzer, P.; Murray, J. S.; Bulat, F., Average local ionization energy: A review. *J. Mol. Model.* **2010**, *16*, 1731-42. DOI: 10.1007/s00894-010-0709-5.
- [38] Murray, J.; Politzer, P., The electrostatic potential: An overview. *WIREs Comp. Mol. Sci.* **2011**, *1*, 153-163, DOI: 10.1002/wcms.19.
- [39] Koopmans, T., Über die zuordnung von wellenfunktionen und eigenwerten zu den einzelnen elektronen eines atoms. *Physica* **1934**, *1*, 104-113, DOI: 10.1016/S0031-8914(34)90011-2.
- [40] Geerlings, P.; De Proft, F.; Langenaeker, W., Conceptual density functional theory. *Chem. Rev.* **2003**, *103*, 1793-1874, DOI: 10.1021/cr990029p.
- [41] Pearson, R. G., Hard and soft acids and bases. *J. Am. Chem. Soc.* **1963**, *85*, 3533-3539, DOI: 10.1021/ja00905a001.
- [42] Pearson, R. G., Application of the principle of hard and soft acids and bases to organic chemistry. *J. Am. Chem. Soc.* **1967**, *89*, 1827-1836, DOI: 10.1021/ja00984a014.
- [43] Anderson, J. S. M.; Melin, J.; Ayers, P. W., Conceptual density-functional theory for general chemical reactions, including those that are neither charge- nor frontier-orbital-controlled. 1. Theory and derivation of a general-purpose reactivity indicator. *J. Chem. Theory Comput.* **2007**, *3*, 358-374, DOI: 10.1021/ct600164j.
- [44] Anderson, J. S. M.; Melin, J.; Ayers, P. W., Conceptual density-functional theory for general chemical reactions, including those that are neither charge- nor frontier-orbital-controlled. 2. Application to molecules where frontier molecular orbital theory fails. *J. Chem. Theory Comput.* **2007**, *3*, 375-389, DOI: 10.1021/ct6001658.
- [45] Politzer, P.; Murray, J. S., An Occam's razor approach to chemical hardness: Lex parsimoniae. *J. Mol. Model.* **2018**, *24*, 332-341, DOI: 10.1007/s00894-018-3864-8.
- [46] Vega, D.; Almeida, D., AIM-UC: An application for QTAIM analysis. *J. Comp. Meth. Sci. Eng.* **2014**, *14*, 131-136, DOI: 10.3233/JCM-140491.